An Optimization-Based Methodology to Predict Digital Human Gait Motion

Hyung Joo Kim*, Emily Horn, Jasbir S. Arora, and Karim Abdel- Malek
Virtual Soldier Research Program,
Center for Computer Aided Design,
The University of Iowa

ABSTRACT

New methods for fast, adaptive motion prediction of a virtual human are proposed and tested. An optimal locomotion for gait-driven motions like pushing, climbing and pick-up/delivery are sought through gradient-based optimization and inverse-dynamics. Such gait-driven motion can be produced by adapting the normal gait motion to the case when a characteristic force is applied, which is called *an applied force*. The applied force is a resistance force for pushing case and an object weight for delivery case. The concept of the zero moment point is modified to assess the dynamic equilibrium of the motion in presence of the applied force. For fast calculation, analytical forms of the cost/constraint gradients are provided. Stepping patterns are specified a priori to ensure the continuity of the cost/constraint function gradients. Also, by varying knots for the B-spline curve approximation, the gait stage durations are optimized.

ABBREVIATIONS

ZMP : Zero Moment Point
CoP : Center of Pressure
BS : Base of Support
GRF : Ground Reaction Force
IGAF : Inertia, Gravity, and Applied Forces

SSP : Single Support Phase
LSS : Single Support on Left foot
RSS : Single Support on Right foot
DSP : Double Support Phase
LDS : Double Support on Left foot
RDS : Double Support on Right foot

LH : Left foot Heel
LT : Left foot Toe
RH : Right foot Heel
RT : Right foot Toe

INTRODUCTION

The objective is to develop methodologies for fast, adaptable dynamic motion prediction of general gait-driven human motion. Past works on gait motion prediction can be sorted by their research focus: 1) to find a dynamically-feasible solution in the shortest amount of time to provide a reference motion for robot control and 2) to find an optimal motion that satisfies various kinematical/physical constraints to fulfill a specified objective.

The works in the first category mostly impose additional equality constraints on gait parameters, such as hip/limb motion or the zero moment point (ZMP: a parameter to assess dynamic equilibrium of walking motion without identification of ground reaction forces) trajectory as a function of time. Such equality constraints are called *artificial constraints* because the gait parameters are arbitrarily chosen by a user rather than being optimized. Those equality constraints are applied a priori to achieve a fast analysis by narrowing down the feasible domain. But it is recommended to minimize the number of artificial constraints used since they may be too restrictive to adapt to changes in the mission goals, the anthropometric data, or the environment (terrain conditions). Azevedo (2004) synthesized a gait motion off-line and applied the simple control law to control a real system. In the off-line motion synthesis, equality constraints on the initial, final, and intermediate positions of the ankle, toe, and hip joints are imposed to ensure obstacle avoidance, static stability, and symmetry of gait stages. Nishiwaki and Kagami (2002) proposed a real-time walking pattern generator to make a humanoid follow specified foot locations on the ground and to maintain a desired zero moment point. In the approach, the initial and final postures, velocity, and arm and foot trajectories are given a priori as equality constraints. Then the horizontal position of the upper body and leg links are modified through an online control system.

* Corresponding author email: hkim@icaen.uiowa.edu

Kuffner (2002) employed a randomized search strategy based on “Rapidly-exploring Random Trees” to find dynamically stable trajectories. In the approach, the collision-free, statically stable, kinematical path is first determined and then adjusted iteratively to a dynamic trajectory. They use an online balance compensation scheme that enforces constraints upon the center of gravity projection and the ZMP trajectory in order to maintain overall dynamic stability.

The works in the second category search for the best solution that achieves user-specified objective. Inverse dynamics combined with optimization is a popular method to solve for optimal human motion. In the framework, the displacement field is first given by optimization. The unbalance of the given displacement field and the force field is evaluated through differential algebraic equation and is imposed as a constraint in the optimization problem. The work by Lo (2002) provides good theoretical background for such human motion prediction strategy even if it does not cover gait motion. He used quasi-Newton nonlinear programming techniques to determine the human motion that minimizes the actuating joint torques. The design variables were the control points for the cubic B-spline approximation of joint angle profiles. Chevallereau (2001) planned a walking and running motion using the Pontryagin Maximum Principle to determine the coefficients of a polynomial approximation for profiles of the pelvis translations and joint angle rotations. Walking is considered a combination of successive single support phases (SSPs) with instantaneous double support phases (DSPs) defined by passive impact. Flying (no support) is composed of stance and flight phases followed by passive impact. Saidouni and Bessonet (2003) solved for cyclic, symmetric gait motion of a nine degree of freedom model that moves in the sagittal plane. A cyclic, symmetric gait motion is composed of repeated gait stages with SSPs and DSPs that are symmetric when the left and right feet change roles. The control points for the B-spline curves along with the time durations for the gait stages (of SSP and DSP) are optimized to minimize the actuating torque energy. By adopting the time durations as design variables both the motion for the single support and for the double support are simultaneously optimized using a global optimization technique. The precedent works using optimization focused on normal human gait motion such that analysis of single gait stage was enough.

For the prediction of general gait-driven motions that are non-cyclic, non-repetitive, and non-symmetric, fast and adaptive motion prediction methods are needed. The fundamental difficulty specific to predicting gait motion resides in the calculation of the ground reaction force on the feet. Proper ground reaction forces should be in coordinate with the inertia forces due to body motion and gravity forces such that they satisfy dynamic equilibrium. Using the ZMP, one can easily check the dynamic equilibrium of a walking motion without calculation of ground reaction force or actuating joint forces. The original concepts date back thirty-five years and recent literature re-examined the concepts either for clarification or extension [Gowami (1999); Vukobratovi and Borovac (2004); Sardin and Bessonnet (2004)]. In this study, the same concept is used but is modified further to incorporate the effect of applied forces on walking. For instance, the motion of pushing a box on a rough floor can be modeled as a biped walking against a resistant, applied force on shoulder. The applied force is equivalent to the constant friction force between the ground and the box and, transferred to the shoulder. The following section will cover the derivation of the modified zero moment point with applied loads.

Since this study develops a new optimization formulation for predicting a general gait-driven motion that is non-cyclic and thus has multiple gait stages, computational cost is higher than that of a single SSP or DSP of a cyclic gait. So, analytical gradients for the cost/constraints are needed to achieve a fast convergence. And the stepping pattern is imposed as an artificial constraint to help quicken convergence. This constraint specifies how many steps the biped takes during the gait motion and the sequence of those steps. We assume that a normal stepping follows the repeated sequence of pattern as: 1) single support on the left foot (LSS); 2) double support with the right foot in the front (RDS) when the right foot heel and the left foot toe are on the ground; 3) single support on the right foot (RSS); 4) double support with left foot in the front (LDS) when the left foot heel and the right foot toe are on the ground. Though the stepping pattern control is an artificial constraint, it is easier to figure out and more general than other artificial constraints such as those on the zero moment trajectory or limb motion. In addition to the stepping pattern control, stage durations are optimized by employing the knots as design variables. The knots determine the B-spline curve approximation of displacement field along with the control points.

ANALYSIS

ZERO MOMENT POINT

This section derives a modified formulation of ZMP that can assess the the dynamic equilibrium of general gait-driven motions in presence of applied force by the relative location of ZMP to a base of support (BS). The BS is a least line segment includes all the foot points on the ground (Γ_{BS} in Figure 1).

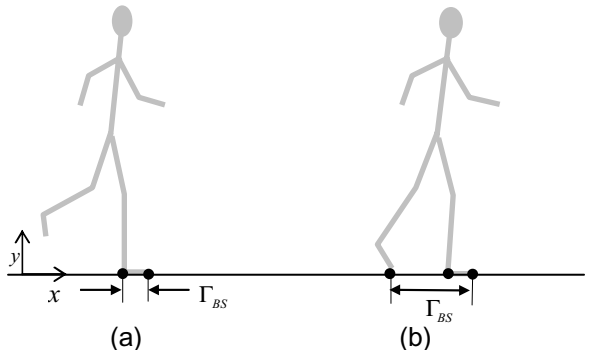

(a) (b)

Figure 1. Base of support (BS): (a) SSP and (b) DSP. The black dot denotes foot-point on ground.

Derivation of Modified Zero Moment Point

Before derivation of modified ZMP, the original concept of ZMP for the case without any applied forces is briefly described in the following section (*italic font*), which refers to the literature by Sardin and Bessonnet (2004).

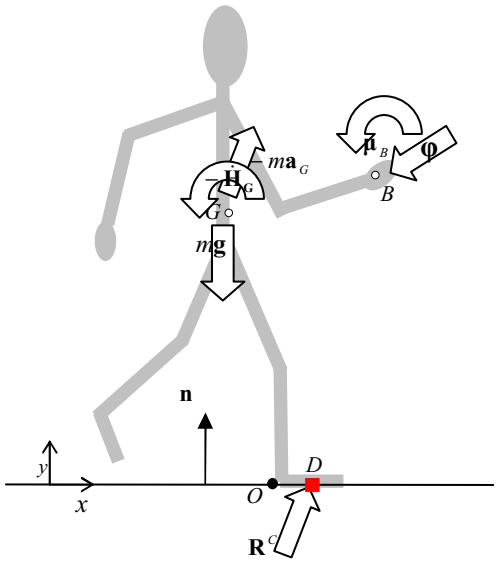

Figure 2. Forces acting on a walking biped. The forces include ground reaction forces, gravity force, inertia forces and applied forces.

Let us sort the forces acting on a walker into two categories: 1) ground contact force on foot; and 2) non-contact forces on body such as inertia, gravity forces. A center of pressure (CoP) is a special point of action for the contact force and, a ZMP for the non-contact forces: The CoP is defined as a point on ground about which the tipping moment by the contact force is zero. The tipping moment is defined as component of the moment that is tangential to ground plane. Meanwhile, ZMP is a point on the ground about which the tipping moment due to non-contact force is zero. For the balance of the tipping moment on the body by the forces, two point CoP and ZMP should coincide each other. Otherwise, when measured at either point, resultant tipping moment by the forces becomes nonzero. And thus, it violates the dynamic equilibrium. Furthermore, by the unilaterality condition of pressure forces (normal component of contact forces to ground plane) that the force between foot and ground is not attractive but repulsive, the CoP lies within the BS. By its coincidence with CoP, the ZMP should also be within the BS.

The expression for a modified ZMP location with applied force acting on the body can be derived as follows. Assume that the applied force is a non-contact force and so the non-contact forces include inertia forces, gravity forces, and applied forces (shortly, IGAF). The resultant force by IGAF is:

$$\mathbf{R}^{IGAF} = m\mathbf{g} - m\mathbf{a}_G + \boldsymbol{\varphi} \tag{1}$$

where m is the total mass of the biped; $\mathbf{g}$ is the acceleration of gravity; G is the center of mass (CoM) of the biped; $\mathbf{a}_G$ is the acceleration of G; $\boldsymbol{\varphi}$ is an applied force at body point B.

The resultant moment by IGAF about the ZMP (D - a red square in Figure 2) is given as:

$$\mathbf{M}_D^{IGAF} = \mathbf{DG}\times m\mathbf{g} - \mathbf{DG}\times m\mathbf{a}_G - \dot{\mathbf{H}}_G + \mathbf{DB}\times\boldsymbol{\varphi} + \boldsymbol{\mu}_B \tag{2}$$

where $\dot{\mathbf{H}}_G$ is the rate of angular momentum at G; $\boldsymbol{\mu}_B$ is applied moment at body point *B*.

Let us consider any point on the ground plane (*O* in Figure 2), then the resultant moment about the point is:

$$\mathbf{M}_O^{IGAF} = \mathbf{OG}\times m\mathbf{g}_G - \mathbf{OG}\times m\mathbf{a}_G - \dot{\mathbf{H}}_G + \mathbf{OB}\times\boldsymbol{\varphi} + \boldsymbol{\mu}_B \tag{3}$$

Then, the Equation (2) is rewritten as:

$$\mathbf{M}_D^{IGAF} = \mathbf{M}_O^{IGAF} - \mathbf{OD}\times\mathbf{R}^{IGAF} \tag{4}$$

From the condition that the tripping moment by the IGAF measured at the ZMP is zero:

$$\begin{aligned}\mathbf{n}\times\mathbf{M}_D^{IGAF} &= \mathbf{n}\times(\mathbf{M}_O^{IGAF} - \mathbf{OD}\times\mathbf{R}^{IGAF}) \\ &= \mathbf{n}\times\mathbf{M}_O^{IGAF} - \mathbf{n}\times(\mathbf{OD}\times\mathbf{R}^{IGAF}) \\ &= \mathbf{n}\times\mathbf{M}_O^{IGAF} - (\mathbf{n}\cdot\mathbf{R}^{IGAF})\mathbf{OD} + (\mathbf{n}\cdot\mathbf{OD})\mathbf{R}^{IGAF} \\ &= \mathbf{0}\end{aligned} \tag{5}$$

where $\mathbf{n}$ is a unit vector that is normal to ground plane and $\mathbf{n}\cdot\mathbf{OD} = 0$. Then, the ZMP *D* is defined by:

$$\mathbf{OD} = \frac{\mathbf{n}\times\mathbf{M}_O^{IGAF}}{\mathbf{n}\cdot\mathbf{R}^{IGAF}} \tag{6}$$

For any walking motion to satisfy dynamic equilibrium, the ZMP should stay within the BS, Γ_{BS} such that:

$$\mathbf{D} \in \Gamma_{BS}, \quad \Gamma_{BS} = \{x \mid \xi_m \le x \le \xi_M\} \tag{7}$$

where ξ_m, ξ_M are the lower and upper bounds of the BS as in Figure 2. The Equation (6) corresponds to the final form of the ZMP location derived in the literature by Sardin and Bessonnet (2004).

Dynamic Stability by ZMP Margin

Generally, the ZMP falls within the boundary of the BS for the dynamic equilibrium. The concept of dynamic stability comes from the notion that a motion is more stable as the distance between the ZMP and the boundary of the BS increases. Assume that the ZMP is actually on the boundary of the BS, and external loads perturb its position such that it crosses the boundary, which is physically invalid. This perturbation will result in the body tipping over or falling unless measures are taken to reposition the BS (i.e. stepping forward or backward).

FORMULATION

The current motion prediction methods are based on gradient-based optimization with inverse dynamics. To maximize the adaptability of this method, this study strives to use the minimum number of artificial constraints: only the stepping pattern constraint is imposed. Other gait parameters like optimal step size, duration of each gait stage, and the initial and final postures are optimized through analysis. The following describes the optimization formulation along with the cost/constraint function definitions.

PROBLEM DEFINITION

The optimization formulation for dynamic motion prediction of human gait is described as follows:

Find:

$$\mathbf{\Theta} = \{\hat{q}_{ki}, \hat{t}_j\} \quad (1 \le i \le n_{ctrl}, 1 \le k \le n_{dof}, 1 \le j \le n_{knot}) \tag{8}$$

that minimize:

$$F(\mathbf{\Theta}) = \int_0^T f^{DS}(\mathbf{q}(\mathbf{\Theta},t), \dot{\mathbf{q}}(\mathbf{\Theta},t), \ddot{\mathbf{q}}(\mathbf{\Theta},t))\, dt\,, \tag{9.a}$$

$$\mathbf{q}(\mathbf{\Theta},t) = \{q_k(\mathbf{\Theta},t) \mid q_k = \sum_i^{n_{ctrl}} \hat{q}_{ki} N_i(t,\hat{t}_j),\ 1 \le k \le n_{dof}\} \tag{9.b}$$

and subject to:

$$H^l(\mathbf{\Theta}) = \int_0^T \tilde{h}^l(\mathbf{q}(\mathbf{\Theta},t), \dot{\mathbf{q}}(\mathbf{\Theta},t), \ddot{\mathbf{q}}(\mathbf{\Theta},t))^2\, dt\,, \quad (1 \le l \le n_{cnstr}) \tag{10.a}$$
$$= 0$$

$$\tilde{h}^l = \begin{cases} h^{EQ}(\ddot{\mathbf{q}}(\mathbf{\Theta},t), \dot{\mathbf{q}}(\mathbf{\Theta},t), \mathbf{q}(\mathbf{\Theta},t)) & \text{(equality)} \\ \max[h^{INEQ}(\ddot{\mathbf{q}}(\mathbf{\Theta},t), \dot{\mathbf{q}}(\mathbf{\Theta},t), \mathbf{q}(\mathbf{\Theta},t), 0] & \text{(inequality)} \end{cases} \tag{10.b}$$

where $\mathbf{\Theta}$ is a set of design variables that includes control points $\hat{q}_{ki}$ s and knots $\hat{t}_j$ s. The parameters n_{ctrl}, n_{dof}, n_{knot} are respectively the number of control points, the degrees of freedom, and the number of knots. $F(\mathbf{\Theta})$ is a cost function that is the integral of dynamic stability, f^{DS} over time. T is the total travel time for motion and $\mathbf{q}(\mathbf{\Theta},t)$ denotes the profiles of joint angle rotations and pelvis translations. The profiles are approximated by cubic B-spline curves in the form of linear combinations of the control points, $\hat{q}_{ki}$, and the corresponding basis functions, $N_i(t,\hat{t}_j)$, as in Equation (9.b). $H^l(\mathbf{\Theta})$ is a square sum of various performance measure violations, $\tilde{h}^l$. The performance measures are sorted into those that are equality conditions, h^{EQ}, and those that are less-than-inequality conditions, h^{INEQ}. The max function in Equation (10.b) filters out the negative values of h^{INEQ} and thus returns only its positive values, which are violations of the performance measures.

STEPPING PATTERN CONTROL

The cost and constraint functions are implicitly governed by stepping pattern control. It specifies which foot-points are in contact with the ground at each gait stage. In the proposed methods, the motion during a single gait stage is approximated by a B-spline curve segment between two consecutive knots (*local time axis*). So, the stepping control can be expressed as function of time and knots instead of gait stage, denoted by $\Psi_C(t,\hat{\mathbf{t}})$:

$$\begin{aligned} &\Psi_C(t,\hat{\mathbf{t}}) = \{f \mid y_\eta(t) = 0 \text{ for } \hat{t}_j \le t < \hat{t}_{j+1}\} \\ &\hat{\mathbf{t}} = \{\hat{t}_j \mid 1 \le j \le n_{knot}\} \end{aligned} \tag{11}$$

where $y_\eta(t)$ is y-coordinate of foot-point η and $\hat{\mathbf{t}}$ is a set of knots. In addition, the stepping pattern control also specifies the leading foot-point $\eta_L(t,\hat{\mathbf{t}})$ and tailing foot-point $\eta_T(t,\hat{\mathbf{t}})$ such that;

$$\begin{aligned} &\eta_T(t,\hat{\mathbf{t}}) = \{\eta \mid \ x_\eta(\mathbf{q}) \le x_\gamma(\mathbf{q}) \text{ for } \forall\, \gamma \in \Psi_C(t,\hat{\mathbf{t}}), \eta \in \Psi_C(t,\hat{\mathbf{t}})\} \\ &\eta_L(t,\hat{\mathbf{t}}) = \{\eta \mid \ x_\eta(\mathbf{q}) \ge x_\gamma(\mathbf{q}) \text{ for } \forall\, \gamma \in \Psi_C(t,\hat{\mathbf{t}}), \eta \in \Psi_C(t,\hat{\mathbf{t}})\} \end{aligned} \tag{12}$$

Then, the upper and lower bounds for BS are given as:

$$\xi^m(\mathbf{q},t) = x_{\eta_T}(\mathbf{q}), \xi^M(\mathbf{q},t) = x_{\eta_T}(\mathbf{q})\,. \tag{13}$$

It is possible to simulate anthropometric walking by imposing practical walking patterns such as toe-off at the beginning of swinging stage and heel landing at the end of it.

TIME DISCRETIZATION

As in Equation (9.a) and (10.a), the cost/constraint function is the integral of the corresponding performance measure over time. Using the trapezoidal rule, the integral term can be replaced by the sum of the

performance measure at discrete time frames, namely *sample time frames*. Here, the sample time frames are chosen to be uniformly-distributed over a local time axis such that:

$$t_{jp} = p\frac{(\hat{t}_{j+1} - \hat{t}_j)}{n_{sample}} + \hat{t}_j \ \ (1 \le p \le n_{smpl}) . \qquad (14)$$

where t_{jp} is the p^{th} sample time frame in the j^{th} local time axis and n_{sample} is the number of sample time frames per a gait stage. Then the cost function can be rewritten as:

$$\begin{aligned} F(\boldsymbol{\Theta}) &= \int_0^T f^{TOP}(\mathbf{q}(\boldsymbol{\Theta},t), \dot{\mathbf{q}}(\boldsymbol{\Theta},t), \ddot{\mathbf{q}}(\boldsymbol{\Theta},t))\, dt \\ &\cong \sum_j \left\{ \sum_p f^{TOP}(\mathbf{q}(\boldsymbol{\Theta},t_{jp}), \dot{\mathbf{q}}(\boldsymbol{\Theta},t_{jp}), \ddot{\mathbf{q}}(\boldsymbol{\Theta},t_{jp}))\Delta t_j \right\}, \\ \Delta t_j &= \frac{(\hat{t}_{j+1} - \hat{t}_j)}{n_{sample}} \end{aligned} \qquad (15)$$

where Δt_j is time step size between sample time frames at the j^{th} gait stage. By letting the sample time frame be a function of knots, such distribution ensures the continuity of cost/constraint gradient over knot changes. Continuity is crucial when providing correct search directions to the gradient-based optimizer.

COST FUNCTION

To minimize the cost function, dynamic stability needs to be maximized. There are two ways to increase dynamic stability by minimizing f^{DS}: (a) increase the margin of ZMP to the border of SR, and (b) increase the support region span.

$$f^{DS}(\mathbf{q},\dot{\mathbf{q}},\ddot{\mathbf{q}},t) = (x_{ZMP}(\mathbf{q},\dot{\mathbf{q}},\ddot{\mathbf{q}}) - \xi^m(\mathbf{q},t))(x_{ZMP}(\mathbf{q},\dot{\mathbf{q}},\ddot{\mathbf{q}}) - \xi^M(\mathbf{q},t)) \qquad (16)$$

where $x_{ZMP}(\mathbf{q},\dot{\mathbf{q}},\ddot{\mathbf{q}})$ is the x-coordinate of ZMP and x_η is x-coordinate of foot-point η.

CONSTRAINTS

There are several types of performance measures for gait motion prediction: 1) joint angle limits, 2) moment equilibrium, 3) no foot-ground slippage, 4) no foot-ground penetration, 5) no foot-ground slippage condition and 6) initial/final conditions for the left foot toe. The constraint condition for joint angle limits is given as follows:

$$q_k^L \le q_k(\boldsymbol{\Theta},t) \le q_k^U \quad \text{for } 1 \le k \le n_{\text{dof}} \quad t \in [0,T] \qquad (17)$$

where q_k is the k^{th} degrees of freedom representing either joint angle or pelvis translation at time frame *t*; and, q_k^L and q_k^U are its upper and lower limits respectively. The conditions for moment equilibrium in two-dimensions is given in inequalities as:

$$\xi^m(\mathbf{q},t) \le x_{ZMP}(\mathbf{q},\dot{\mathbf{q}},\ddot{\mathbf{q}}) \le \xi^M(\mathbf{q},t) . \qquad (18)$$

The constraint for *no foot-ground slippage* ensures that the horizontal velocity of the foot-points contacting the ground contact is zero. The condition is given as follows:

$$\dot{x}_\eta(\mathbf{q},t) = 0 \ \text{ for } \eta \in \Psi_C \qquad (19)$$

where $\dot{x}_\eta$ denotes the velocity in x-direction of the foot-point η. The constraint for *no ground penetration* imposes the condition that the foot-points that are not in ground contact stay above ground level. This constraint is stated as follows:

$$y_\eta(\mathbf{q},t) \ge 0 \ \text{ for } \eta \in \Psi_F(t,\hat{\mathbf{t}}) \qquad (20)$$

where $\Psi_F (= \Psi_C{}^C)$ is the set of foot-points that are not in ground contact. The *initial/final conditions* for the left foot are stated as follows:

$$\begin{aligned} x_{LFT}(\mathbf{q},t=0) &= x_{IC} \\ x_{LFT}(\mathbf{q},t=T) &= x_{FC} \end{aligned} \qquad (21)$$

where x_{LFT} is the x-coordinate of the left foot-toe. The values x_{IC} and x_{FC} are the locations at the initial and final time frames.

NUMERICAL EXAMPLES

HUMAN LINKAGE MODEL

The proposed motion prediction methods are tested for practicality and robustness by using a simpler human model. This human body is modeled as multi-linkage system that is planar and consists of 13 DOF. There are 2 degrees of freedom for global translation of the pelvis $\{x, y\}$ and 11 DOF for the relative joint angles $\{\theta_1, \theta_2, \ldots, \theta_{11}\}$. All joint displacements are defined in the Sagittal plane. The mass of each body link is concentrated at its center of gravity (Table 1) and the rotational moment of inertia is neglected. Since the virtual human does not have a neck and head, theirs masses are combined to a trunk mass. The trunk orientation, or sway motion, is measured by the angle θ_7, which is relative to the global vertical y-axis. The other angles are measured relative to the angle of upper body link that is closer to the pelvis as illustrated in Figure 3.

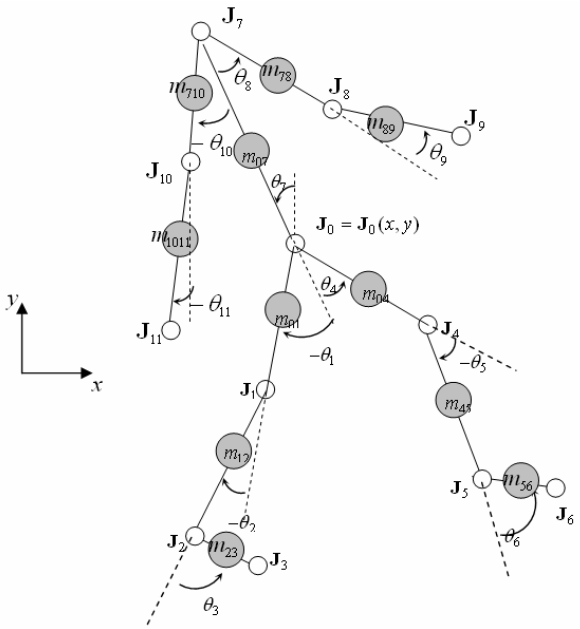

Figure 3. The 13-DOF human linkage model; there are two degrees of freedom for pelvis translation and eleven degrees of freedom for the relative joint angles.

Table 1. The mass distribution of body [Winter, D. A. (1979)].

$m_{23}/\overline{m}$, $m_{56}/\overline{m}$ (foot)	1.45 (%)
$m_{12}/\overline{m}$, $m_{45}/\overline{m}$ (shank)	4.65
$m_{01}/\overline{m}$, $m_{04}/\overline{m}$ (thigh)	10.0
$m_{07}/\overline{m}$ (trunk+head+neck)	57.8
$m_{710}/\overline{m}$, $m_{78}/\overline{m}$ (upper arm)	2.8
$m_{1011}/\overline{m}$, $m_{89}/\overline{m}$ (fore arm+hand)	2.2

($\overline{m}$ is a total mass=80 kg)

PUSHING MOTION

The example is for simulation of a biped pushing a load while walking. The load is modeled as a constant force acting on the shoulder and in the opposite direction as the movement. The resistant force is caused by the friction between the object being pushed and the ground. To illustrate the adaptability of this dynamic motion simulation two cases are shown. The first case uses an external force of 250 N (Figure 4) and the second case uses an external force of 500 N (Figure 5). The stepping pattern control is specified as in Table 1. The initial and final conditions are given as positions of the left foot-points and are two meters away.

Table 2. Stepping Pattern

Gait stage	Ψ_C	η_T	η_L
1 (LDS)	LH, RT	RT	LH
2(LSS)	LH, LT	LH	LT
3(RDS)	LT, RH	LT	RH
4(RSS)	RH, RT	RH	RT
5(LDS)	LH, RT	RT	LH
6(LSS)	LH, LT	LH	LT
7(RDS)	LT, RH	LT	RH
8(RSS)	RH, RT	RH	RT
9(LDS)	RT, LH	RT	LH

(LH= left foot heel, LT= left foot toe, RH=right foot heel and RT= right foot toe)

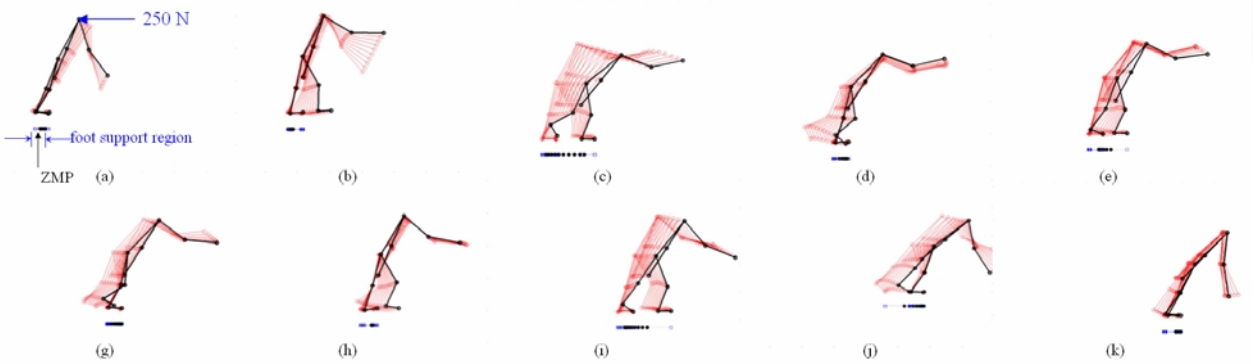

Figure 4. Pushing an object (resistance force = 250 N).

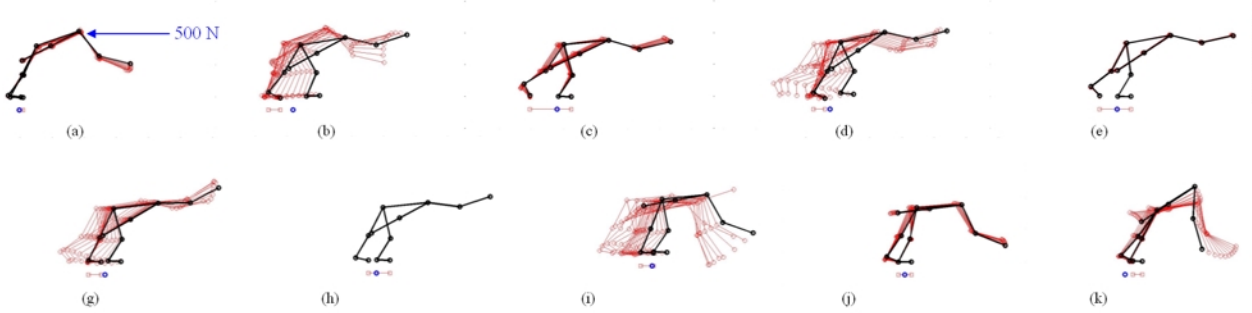

Figure 5. Pushing an object (resistance force = 500 N).

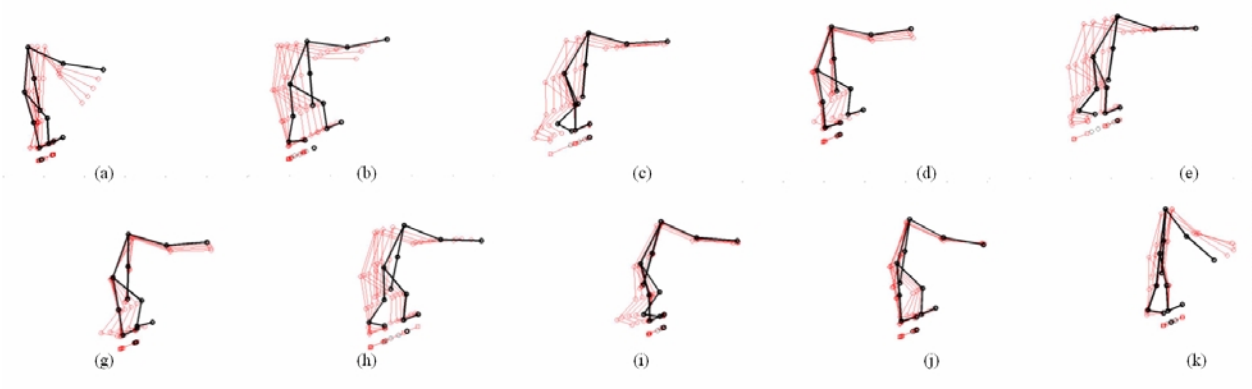

Figure 6. Climbing on the slope with α =0.5 (rad).

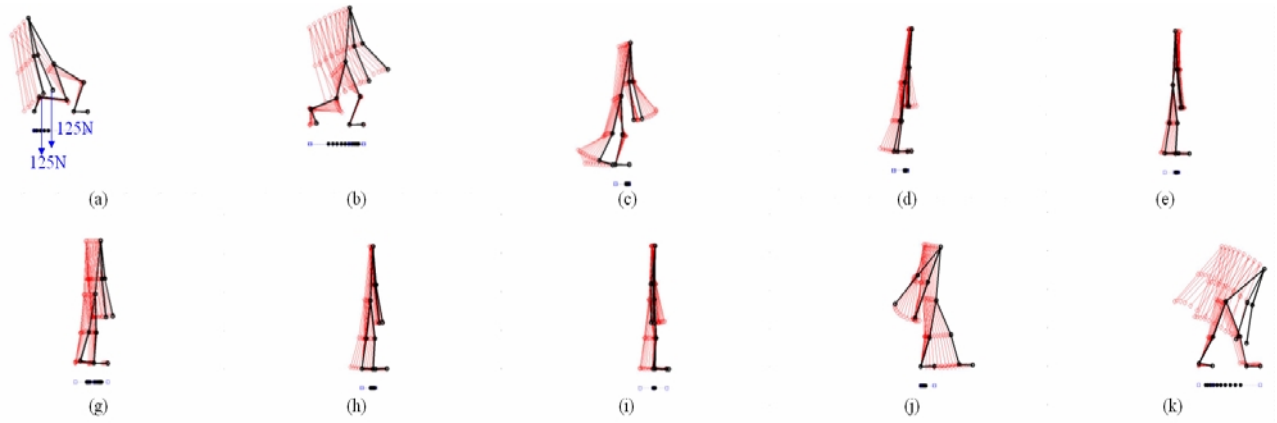

Figure 7. Pick-up and delivery

CLIMBING

The predicted climbing motion is actually very similar to that in pushing motion (Figure 6). In climbing, the tangential component of gravity to the slope acts in the opposite direction as motion just as the external force did in the pushing example. Since the friction force is assumed large enough in this study, the human will not slip along the slope in the Figure. But friction is very important in practices when the normal component of the IGEF to the slope becomes smaller as the slope increases and, the friction force may not be large enough to prevent slipping.

PICK-UP AND DELIVERY

The third example shows the lifting, carrying, and delivery of an object weighing 250 N (Figure 7). To simulate the picking-up motion and delivery, the hand locations are specified at initial and final time frames instead of foot locations. The object weight is applied as a constant external force acting downward on the hands. The magnitude of this external force is 125 N applied to each hand.

The posture for picking up the object is shown in Figure 7(a). Although the optimal solution results in the person bending backward to pick up the object this is not a solution that is true to life. Bending backward results in a solution with maximum dynamic stability, but it is impractical in two ways: 1) is the box is being picked up by two hands this solution may result in the box and trunk colliding and 2) in real-life visibility may have just as much consideration as stability. A person assumes a posture that allows him/her to see the object being lifted. Another issue to consider when carrying an object is the inertia force of the object. Since when the object is heavy its inertia forces may be considerable.

CONCLUSION

New gradient-based optimization methods are proposed to achieve fast, adaptive prediction of general human gait-driven motions. The methods solve for the optimal displacement field and gait durations that satisfy all the constraints given and achieve a certain objective. These constraints include keeping joints within their limits; maintaining dynamic equilibrium; not allowing the feet to slip on the ground; not allowing the feet to penetrate the ground; and meeting the initial and final position constraints. The objective is to maximize the dynamic stability of motion.

The major contributions of this study to the field of motion prediction are: 1) the extension of the ZMP concept to the case of walking under applied forces; 2) the formulation of a motion prediction method that is suitable for gradient-based optimization by controlling the stepping pattern and using variable knots; 3) the development of a fast, adaptable motion prediction program that predicts general gait-driven human motions.

The current development of this dynamic motion prediction program is aimed at extending the framework of motion prediction to three-dimensions. It is expected that the lateral stability may have more influence on the choice of optimal motion than the stability in forward direction. This is because the stability margin of ZMP in the lateral direction is smaller than that in forward direction.

ACKNOWLEDGMENTS

This research is funded by the US Army TACOM project: Digital Humans and Virtual Reality for Future Combat Systems (FCS) (Contract No.: DAAE07-03-Q-BAA1).

REFERENCES

Azevedo, C., Poignet, P. and Espiau, B. (2002), "Moving horizon control for biped robots without reference trajectory", *Proceedings of the 2002 IEEE, international conference on robotics &Automation*, Washington, DC, 2762-2767.

Bessonnet, G., Sardain, P. and Chesse, S. (2002), "Optimal motion synthesis- dynamic modeling and numerical solving aspects," *Multibody System Dynamics*, 8(3), 257-278.

Chevallereau, C. and Aousin, Y. (2001), "Optimal reference trajectories for walking and running of a biped robot," *Robotica,* 19, 557-569.

Goswami, A. (1999), "Postural stability of biped robots and the foot rotation indicator point," *International Journal of Robotics Research,* Vol. 18(6), pp. 523-533.

Kuffner, J., James, J., Kagami, S., Nishiwaki, K. Inaba, M. and Inoe H. (2002), "Dynamically-stable motion planning for humanoid robots," *Autonomous Robots*, 12, 105-118.

Lo, J., Huang, G. and Metaxas, D. (2002), "Human motion planning based on recursive dynamics and optimal control techniques," *Multibody System Dynamics,* 8, 433-458

Nishiwaki, K. and Kagami, S. (2002), "Online generation of humanoid walking motion based on a fast generation method of motion pattern that follows desired ZMP," *IEEE International Conference on Intelligent Robots and Systems*, 3, 2684-2689

Rostami, M. and Bessonnet, G. (2001), "Sagittal gait of a biped robot during the single support phase. Part2: optimal motion," *Robotica*, 19(3), 241-253.

Saidouni, T. and Bessonnet, G. (2003), "Generating globally optimized sagittal gait cycles of a biped robot," *Robotica*, 21(2), 199-210.

Sardain, P. and Bessonnet, G. (2004), "Forces acting on a biped robot. Center of pressure- zero moment point", *IEEE Transations on systems, man and cybernetics- Part A: Systems and Humans*, Vol. 34(5), pp. 630-637.

Vukobratovi , M. and Borovac, B. (2004), "Zero-moment point – thirty five years of its life," *International Journal of Humanoid Robotics*, Vol 1 (1), pp. 157-173.

Winter, D. A. (1979). *Biomechanics of human motion*. New York: Wiley.

CONTACT

Corresponding author: Hyung Joo Kim, Ph. D. Working as a postdoctoral research associate at Virtual Solider Research (VSR), Center for Computer Aided Design (CCAD), The University of Iowa, Iowa City, IA 52242, USA. Tel: 319-936-9248, Fax: 319-384-0542, E-Mail: hkim@icaen.uiowa.edu